agronomy

Article

Responses of Soil Labile Organic Carbon on Aggregate Stability across Different Collapsing-Gully Erosion Positions from Acric Ferralsols of South China

Xian Tang [1,2,†], Yousef Alhaj Hamoud [3,†], Hiba Shaghaleh [4], Jianrong Zhao [2], Hong Wang [2], Jiajia Wang [5], Tao Zhao [6], Bo Li [1] and Ying Lu [1,*]

1 College of Natural Resources and Environment, South China Agricultural University, Guangzhou 510642, China; tangxian@ahstu.edu.cn (X.T.); boli@scau.edu.cn (B.L.)
2 College of Natural Resources and Environment, Anhui Science and Technology University, Chuzhou 233100, China; zhaojr@ahstu.edu.cn (J.Z.); hongw_21@163.com (H.W.)
3 College of Hydrology and Water Resources, Hohai University, Nanjing 210098, China; yousef-hamoud11@hotmail.com
4 College of Environment, Hohai University, Nanjing 210098, China; hiba-shaghaleh@hotmail.com
5 Anhui Provincial Key Laboratory of Nutrient Cycling, Resources & Environment, Institute of Soil and Fertilizer, Anhui Academy of Agricultural Sciences, Hefei 230031, China; 15155155551@163.com
6 Aerospace Environmental Engineering Co., Ltd., Tianjin 300301, China; 2516209097@tju.edu.cn
* Correspondence: luying@scau.edu.cn; Tel./Fax: +86-020-8528585
† These authors contributed equally to this work.

Abstract: Soil labile organic carbon (LOC) is a valuable and sensitive parameter of the changes in soil carbon (C) pools and further affects soil structural stability. However, the influences of soil-aggregate stability on LOC fractions under erosion conditions are still unclear, especially under the collapsing gully area of south China. Soils of five positions of collapsing gully erosion, including the upper catchment (UC), collapsing wall (CW), colluvial deposit (CD), scour channel (SC) and alluvial fan (AF) from Acric Ferralsols were investigated and sampled. Soil aggregate stability and LOC fractions were measured and analyzed. Soil water-stable aggregate and passive C (passive-C) contents significantly increased by 67–76% and 8.7–13.0% at the UC, CW, CD and SC positions, respectively, while soil labile C (labile-C) content was lower at these positions as compared to the AF position ($p < 0.05$). Moreover, the UC position's soil C pool management index (CPMI) significantly increased by 37–40% compared to CW, CD, SC and AF soils, indicating that the soil of the UC position had a more stable C pool due to its stronger structural stability. SOC, silt, and amorphous iron oxide (Fea) contents significantly contributed to aggregate stability. We demonstrated that the depletion of soil aggregate stability could result in the decreases in soil LOC fractions, while soil properties of the OC but not the LOC pool regulated aggregate stability and thus affected soil structure across different collapsing gully erosion positions in the subtropical Acric Ferralsols region of south China. This study contributes to developing strategies to prevent soil erosion and improve global C cycle and soil quality, which could be beneficial to strengthen soil and water conservation, and improve soil fertility (e.g., SOC) and vegetation recovery, such as tea and tobacco.

Keywords: soil LOC; C pool management index; collapsing gully erosion; aggregate stability; Acric Ferralsols

Citation: Tang, X.; Alhaj Hamoud, Y.; Shaghaleh, H.; Zhao, J.; Wang, H.; Wang, J.; Zhao, T.; Li, B.; Lu, Y. Responses of Soil Labile Organic Carbon on Aggregate Stability across Different Collapsing-Gully Erosion Positions from Acric Ferralsols of South China. *Agronomy* **2023**, *13*, 1869. https://doi.org/10.3390/agronomy13071869

Academic Editors: Lianghuan Wu, Xiaochuang Cao, Wenhai Mi and Qingxu Ma

Received: 12 June 2023
Revised: 7 July 2023
Accepted: 12 July 2023
Published: 14 July 2023

1. Introduction

Soil organic carbon (SOC) is a key index for assessing soil fertility and function, which is crucial to the long-term sustainable development of agricultural ecosystems [1,2]. However, soil labile organic carbon (LOC) is considered a main indicator for SOC-content measurement and has a great impact on soil quality due to its high susceptibility to oxidation and decomposition, which has vital effects on the global carbon cycle [3–5]. Soil LOC has been shown to correlate positively with soil aggregate stability, particularly macroaggregate stability [5,6]. Moreover, stable LOC fractions have turnover durations in soils of thousands of years; however, it is not influenced by short-term tillage [7], except for soil erosion and aggregate stability. Thus, assessing soil erosion's impacts on soil LOC fractions and the relationship between soil LOC and aggregates is very helpful in understanding the SOC cycle and dynamics in natural systems.

Soil aggregate, as a fundamental component of soil structure, has an essential influence on soil ecological processes and organic C stability, which is critical for enhancing soil fertility by preventing soil erosion, regulating the rate of infiltration and recycling nutrients [8,9]. Furthermore, soil aggregate can physically protect SOC from mineralization because aggregates restrict the availability of organic materials, including microbes, enzymes and proteins [10]. However, soil aggregate structure is destroyed in a collapsing gully environment, resulting in a declining aggregate stability and nutrient loss, including LOC fractions [11–13]. Additionally, the disintegration of soil aggregates caused by raindrop impact and surface discharge can accelerate the release of protected organic C in aggregates. The liberated organic C can then be transported and deposited with soil aggregate particles [14,15]. These processes can hasten the decomposition of organic C due to the loss of protection from macroaggregates [16]. The priority-transported and -deposited organic C is regarded as LOC fractions, thus further decreasing the stability of the LOC pool in the original sites [17]. Therefore, the effects and relationships of aggregate stability on the changes in soil LOC pool under the collapsing-gully erosion condition need to be further investigated in south China, which would be helpful for providing applicable management patterns to balance the C pool and control erosion for improved soil quality and the provision of soil functions.

Due to its chronic and severe impacts on the ecosystem and environment, particularly subtropical the Acric Ferralsols zone of south China, collapsing gully erosion has emerged as the greatest challenge to the development of global soil sustainability [18,19]. During the collapsing gully process, a mass of sediments generate and flow out through the SC, further cover the cultivation layer of AF cropland, and, thus, have negative feedback on the soil-aggregate stability and nutrients [20–23]. Moreover, collapsing gully erosion profoundly influences nutrient dynamics and aggregate stability, resulting in the losses of soil materials and soil degradation, further affecting soil LOC pool and biogeochemical cycles [24,25]. Thus, among all the soil properties, soil LOC is important in affecting C pool and aggregate stability, maintaining soil quality, and regulating global climate change [26–28]. However, the link between soil LOC fractions and aggregate stability during collapsing gully erosion remains unclear. Thus, the effect of soil LOC fractions on soil-aggregate size distributions related to soil erosion need to be further assesses.

Previous studies have proved that soil erodibility factor (K) and structural stability index (St), which are calculated by empirical equations based on soil-particle composition and organic C content, are frequently used as essential parameters to assess soil structure stability and credibility, and thus, better understand soil anti-erosion capability [29,30]. That being said, such indices are impacted by fundamental soil properties (e.g., SOC), indicating that soil structure stability can be interlinked with many soil properties; however, these properties could significantly change if the soil were to suffer from collapsing gully erosion [31,32]. Furthermore, collapsing gully erosion affects soil-aggregate stability directly by increasing the losses of runoff, binding materials and nutrient contents, and indirectly by affecting other soil properties, including soil porosity, water-holding capacity and bulk density [33]. Moreover, preventing and controlling soil erosion are beneficial to boosting soil fertility and crop yield (e.g., wheat, tea and tobacco) [34]. Therefore, it is vital to demonstrate the effect of collapsing gully erosion on soil-aggregate stability, LOC and their interaction.

Understanding the role of and change in soil LOC in aggregate formation related to collapsing gully erosion is extremely important. Thus, the goal of this research was to look into the distributions and differences in soil LOC fractions and aggregate size and elucidate the correlations between soil LOC pool indexes and aggregate stability parameters at various collapsing gully erosion positions. We hypothesized that soil LOC fractions and organic C pool were significantly different among collapsing-gully erosion positions and strongly influenced aggregate stability in the south subtropical Acric Ferralsols region.

2. Materials and Methods

2.1. Study Area and Soil Sampling

This research site was in Deqing country, Zhaoqing city (111°51′ E, 23°14′ N), Guangdong Province, China, which is a low-latitude location with a subtropical monsoon climate, abundant heat, abundant rainfall and very short frost period. According to the average data from the years 2000~2021, the average annual temperature, precipitation and sunlight duration in this location are approximately 22.2 °C, 1505.4 mm and 1697.1 h, respectively [35]. The sampling location is in the Southeast Sham Chung Soil and Water Conservation Monitoring Station at Maxu town of Deqing county (111°50′ E, 23°10′ N). With a vegetation coverage of 41%, the plant community was dominated by *Schima superba Gardn. Et Champ.*, *Baeckea frutescens* L., and *Dicranopteris dichotoma (Thunb.) Berhn*. This site was a typical collapsing gully. The gully belonged to the arc gully with two erosion grooves. The channel's average depth, width and length was 3, 1.8 m and 16 m, respectively. The channel's greatest width was 5.2 m. The height of the wall behind the collapsing wall was 5 m, and the side wall was 3.6 m. The entire collapsing gully area was 136 m^2 [36]. The collapsing gully was mainly developed from the granite weathering residual hills with the bedrock of Yanshanian biotite granite, and the weathering crust ranged from 30–60 m. Currently, it is in the prime of life with large-scale and vigorous erosion [35]. The soil of this area is classified as Acric Ferralsols derived from granite [37].

Five positions of collapsing gully erosion were examined in November 2019 (Figure 1) and named the upper catchment (UC), collapsing wall (CW), colluvial deposit (CD), scour channel (SC), and alluvial fan (AF) by Wei et al. (2021) [13]. Soil sampling was described by Tang et al. (2022) [38]. Finally, five mixed soil samples and fifteen undisturbed soil cores were obtained and transported to the laboratory. All samples were manually broken into $\leq$ 5 mm soil blocks and then air-dried indoors before divided into two sections: one for the analysis of the soil's basic properties, which was ground to pass through a 2 mm and 0.15 mm sieve, respectively, and the remaining for soil aggregate contents and stability analysis.

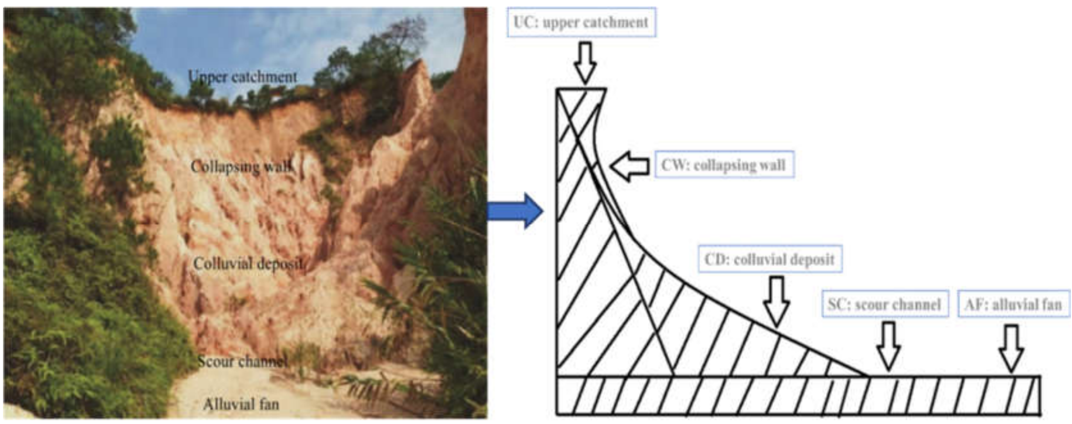

Figure 1. Location of each position of soil erosion under collapsing-gully erosion from Acric Ferralsols of south China.

2.2. Soil Basic-Property Analysis

Soil bulk density (BD), capillary porosity (CP) and non-capillary porosity (NP) were evaluated using the cutting ring method [38]. Soil sand, silt and clay contents were measured using the pipette method [38]. The soil organic carbon (SOC) content was obtained using a wet digestion technique with potassium dichromate [39]. The Kjeldahl technique was used to determine the total nitrogen (TN) content of the soil [39]. The dithionite-citrate-bicarbonate-phenanthroline colorimetric approach was used to estimate soil free iron (Fef), and soil amorphous iron oxide (Fea) was determined by ammonium oxalate extraction and the phenanthroline colorimetric method [38].

2.3. Analysis of Soil-Aggregate Stability

The size content of soil aggregate was measured using a wet-sieving technique [40], which separated aggregates using the modified approach described by Elliott et al. (1986) [41]. The detailed procedures of soil-aggregate analysis were described by Tang et al. (2022) [38]. Finally, four aggregate sizes (2–5, 0.25–2, 0.053–0.25 mm and < 0.053 mm) were collected and dried at 50 °C before being weighed to calculate aggregate stability parameters [42,43]. In addition, we further determined SOC, TN, Fef and Fea contents in the four aggregate sizes (Table S1).

The percentage of soil-aggregate size fractions (PSA_i) and the percentage content of >0.25 mm water-stable aggregate (WSA) were calculated as follows [44], respectively:

$$PSA_i(\%) = w_i \tag{1}$$

$$WSA\ (\%) = 100 - \sum_{i=3}^{4} w_i \tag{2}$$

where i denotes the number of aggregate sizes, and w_i denotes the proportion of the total aggregates in the i size. The percentages of 2–5, 0.25–2, 0.053–0.25 mm and <0.053 mm aggregates were represented as PSA_1, PSA_2, PSA_3 and PSA_4, respectively.

The mean weight diameter (MWD) and geometric mean diameter (GMD) were computed as follows [45,46], respectively:

$$MWD\ (mm) = \frac{\sum_{i=1}^{n}(x_i w_i)}{\sum_{i=1}^{n} w_i} \tag{3}$$

$$GMD\ (mm) = \exp\frac{\sum_{i=1}^{n}(w_i \mathrm{In} x_i)}{\sum_{i=1}^{n} w_i} \tag{4}$$

where i denotes the total number of fractions, w_i denotes the percentage of the total aggregates in the i size, and x_i denotes the mean diameter of the i size.

The soil structural stability index (St) and soil erodibility factor (K) were estimated as follows [47,48]:

$$St\ (\%) = 100 \times \frac{1.724SOC}{clay + silt} \tag{5}$$

$$K\ (t\,hm^2\,h\,MJ^{-1}mm^{-1}hm^{-2}) = \left\{ \begin{array}{c} \left[0.2 + 0.3\exp^{-0.0256sand\left(1-\frac{silt}{100}\right)}\right] \times \left(\frac{silt}{clay+silt}\right)^{0.3} \\ \times\left(1 - \frac{0.25SOC}{SOC + \exp^{3.72-2.95SOC}}\right) \times \left(1 - \frac{0.7SN1}{SN1 + \exp^{22.9SN1-5.51}}\right) \end{array} \right\} \times 0.51575 - 0.01383 \tag{6}$$

$$SN1 = 1 - \frac{sand}{100} \tag{7}$$

2.4. Soil-LOC-Fraction Analysis

Soil LOC fractions were measured by the $KMnO_4$ oxidation approach [49]. First, a 0.15 mm sample with the mass of approximately 15 mg C and a 25 mL $KMnO_4$ solution (33, 167 mM L^{-1} and 333 mM L^{-1}, respectively) were added to a 100 mL centrifuge tube, followed by three blank controls without soils; second, the soil suspension was shaken for 60 min with 250 r min^{-1} before being centrifuged for 5 min at 2000 r min^{-1}; third, the supernatant was collected and diluted to 1:250 with deionized water before the absorbance of the diluted solution was determined at 565 nm to acquire sample absorbance; finally, using absorbance as the Y-axis and concentration as the X-axis, the regression equation calculated sample concentration (C_{sample}, mM L^{-1}) and blank control concentration (C_{ck}, mM L^{-1}). The findings were represented as mg C g $soil^{-1}$, assuming that 1 mM MnO^{4-} oxidizes 0.75 mM or 9 mg C. In addition, the quantities of the remaining oxidized and unoxidized organic C were classified as SOC's labile and non-labile components, respectively [50]. Thus, all four distinct LOC fractions were obtained [51,52]: (i) high-labile organic C (HLOC), organic C oxidized with 33 mM L^{-1} $KMnO_4$; (ii) moderately labile organic C (MLOC), organic C oxidized with 167 mM L^{-1} $KMnO_4$; (iii) less-labile organic C (LLOC), organic C oxidized with 333 mM L^{-1} $KMnO_4$; (iv) non-labile organic C (NLOC), the difference of SOC and organic C oxidized with 333 mM L^{-1} $KMnO_4$. Thus, soil LOC fractions were calculated as follows [53]:

$$\text{Soil LOC } (\text{LLOC, HLOC, MLOC or NLOC, g kg}^{-1}) = \frac{(C_{sample} - C_{ck}) \times 25 \times 250 \times 9}{M \times 1000} \tag{8}$$

where C_{sample} was the sample concentration (mM L^{-1}); C_{ck} was the blank control concentration (mM L^{-1}); and M was the soil mass (g).

Additionally, soil labile-C pool was calculated by the sum of the high-labile fraction (HLOC), moderately labile fraction (MLOC) and less-labile fraction (LLOC), while the non-labile fraction (NLOC) was defined as soil passive-C pool [2,53].

2.5. Statistical Analysis

To assess the variance of the soil C pool, woodland soil without erosion in the adjacent position of the collapsing hill was used as the reference (the SOC content of the referenced soil was 12.65 g kg^{-1}, and the soil C pool liability (L) was 0.45).

Soil C pool management index (CPMI) was computed as follows [53]:

$$\text{CPMI } (\%) = \text{CPI} \times \text{LI} \times 100 \tag{9}$$

where CPI represented the C pool index and LI represented the C pool liability index.

In addition, soil CPI, LI and L values were determined using the following formulae [53], respectively:

$$\text{CPI} = \frac{SOC_T}{SOC_R} \tag{10}$$

$$\text{LI} = \frac{L_T}{L_R} \tag{11}$$

$$L_T \text{ or } L_R = \frac{LLOC_T \text{ or } LLOC_R}{NLOC_R \text{ or } NLOC_R} \tag{12}$$

where SOC_T and SOC_R represent the SOC contents (g kg^{-1}) in soils of erosion positions (UC, CW, CD, SC, and AF) and the reference, respectively; L_T and L_R represent the C pool liability in the soil of erosion positions and the reference, respectively; $LLOC_T$ and $LLOC_R$ represent the less-labile oxidizable organic C content (g kg^{-1}) in soils of erosion positions and the reference, respectively; and $NLOC_T$ and $NLOC_R$ represent the non-labile oxidizable organic C content (g kg^{-1}) in soils of erosion positions and the reference, respectively.

All data were subjected to variance analysis using SPSS 24.0 (IBM SPSS Corporation, New York, USA). All illustrations were created in Origin 2023 (OriginLab Crop, Northampton, MA, USA). Significant differences in mean values were compared using the least significant difference (LSD) tests and the Duncan test ($p \leq 0.05$). Principal component analysis (PCA) and path analysis were performed to explore the key factors regulating aggregate stability under different erosion positions using Origin 2023. Redundancy analysis (RDA) was used to ascertain the correlations among soil-aggregate stability, LOC fractions and soil characteristics by Canoco 5.0 (Canoco, New York, NY, USA).

3. Results

3.1. Physicochemical Properties in Bulk Soils along Erosion Positions

Table 1 shows the SOC content ranging from 1.3–26.2 g kg^{-1} among erosion positions. Compared with UC, SOC content strongly decreased by 91.0–95.2% among the lower erosion positions, and SC had the lowest SOC value. Soil TN content was 0.02–0.36 g kg^{-1} with a significant decrease of 84.1–95.0% at the CW, CD, SC and AF positions compared to UC (Table 1). Furthermore, compared with UC, BD was significantly higher at the CD and SC and lower at the CW and AF positions. At the same time, CP was significantly higher among the rest of the erosion positions. Compared to UC, soil Fef was significantly decreased by 43.0–57.6% among the lower erosion positions, and AF had the lowest Fef content.

Table 1. Basic physical and chemical parameters of the soils at the research locations (mean ± SE).

Erosion Position	BD (g cm^{-3})	CP (%)	Clay (%)	Silt (%)	Sand (%)	SOC (g kg^{-1})	TN (g kg^{-1})	Fef (g kg^{-1})	Fea (g kg^{-1})
UC	1.07 ± 0.10b	36.0 ± 1.5c	49.9 ± 0.50a	9.38 ± 0.36c	40.8 ± 0.39d	26.2 ± 0.3a	0.36 ± 0.01a	56.4 ± 0.2a	2.50 ± 0.08b
CW	0.99 ± 0.03c	45.4 ± 5.0b	11.5 ± 0.19c	17.2 ± 0.6b	71.3 ± 0.6c	2.36 ± 0.06b	0.06 ± 0.00b	32.1 ± 1.03b	6.14 ± 0.13a
CD	1.40 ± 0.05a	38.5 ± 1.0b	7.63 ± 0.15e	6.67 ± 0.09d	85.7 ± 0.2a	1.69 ± 0.09c	0.03 ± 0.01c	29.2 ± 0.1c	2.23 ± 0.03c
SC	1.36 ± 0.02a	38.8 ± 0.1b	9.15 ± 0.22d	9.09 ± 0.51c	81.8 ± 0.3b	1.26 ± 0.03d	0.02 ± 0.00c	28.7 ± 0.1d	2.74 ± 0.07b
AF	1.03 ± 0.00c	62.9 ± 0.7a	21.3 ± 0.2b	54.5 ± 0.5a	24.3 ± 0.6e	1.67 ± 0.04c	0.03 ± 0.00c	23.9 ± 0.1e	1.08 ± 0.04d

UC, upper catchment; CW, collapsing wall; CD, colluvial deposit; SC, scour channel; AF, alluvial fan; SE is the standard error. BD, bulk density; CP, capillary porosity; SOC, soil organic carbon; TN, total nitrogen; Fef, free iron; Fea, amorphous iron oxide. Different lowercase letters indicate different erosion positions are significant at $p < 0.05$.

In contrast, the Fea content was higher at the CW and lower at the CD and AF positions, respectively. Moreover, soil clay content significantly decreased by 57.4-84.7% among the lower erosion positions compared to the UC position, and CD had the lowest clay value. On the contrary, silt content was higher at the CW and AF and lower at the CD positions than at UC. In comparison, sand content was significantly higher at the CW, CD, and SC and lower at the AF positions than at UC (Table 1).

3.2. Distributions of Soil-Aggregate Size and Stability along Erosion Positions

There were significant differences in aggregate soil stability, size distribution, and erodibility across the different erosion positions (Figures 2 and 3, $p < 0.05$). The content of PSA_1 was dominant in all aggregate fractions, with the contents of 70.4–84.9% at the UC, CW, CD, and SC positions, but the percentage of microaggregates (<0.25 mm aggregates, including PSA_3 and PSA_4) were dominant in all aggregate fractions, with the contents of 36.6–40.8% at the AF position (Figure 2). Furthermore, the PSA1 and PSA_2 contents were significantly higher at the UC, CW, CD, and SC positions than the AF position, while the PSA_3 and PSA_4 contents were significantly higher at AF than the UC, CW, CD, and SC positions (Figure 2). Additionally, the WSA content was significantly decreased by 1.82–77.1% among the lower erosion positions except for CD, compared to UC position (Figure 2).

Compared with UC, the MWD and GMD values were significantly higher with 0.44–2.42 mm and 0.83–2.53 mm at the CW and AF positions, respectively ($p < 0.05$), but there was no significant change at the UC, CD and SC positions (Figure 3a,b, $p > 0.05$). Furthermore, the value of St was significantly decreased by 73.2–95.0% among the lower erosion positions compared to the UC position, and AF had the lowest St value (Figure 3c, $p < 0.05$). On the contrary, the value of soil K was significantly increased by 55.6–181.5% at the CW and AF positions, while it significantly decreased by 16.9% at the CD position compared to the UC position (Figure 3d, $p < 0.05$). Among all erosion positions, the MWD, GMD, WSA, and St changes had a similar trend, except for K (Figure 3).

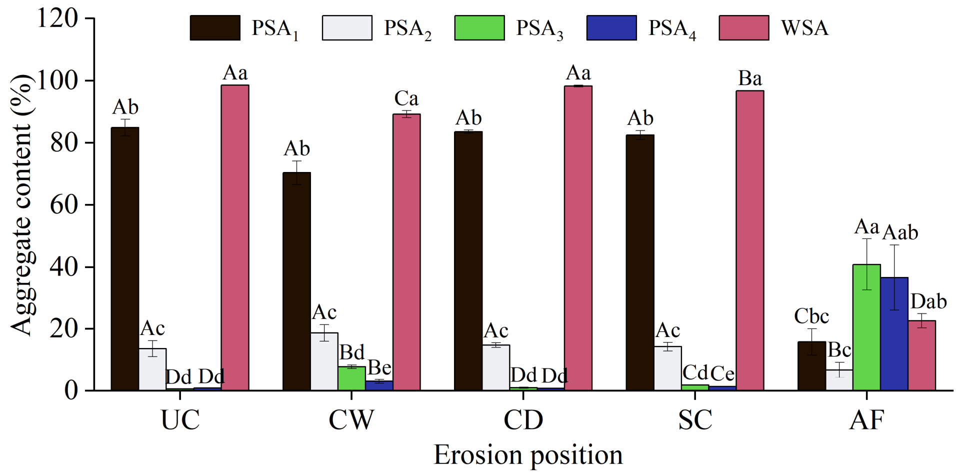

Figure 2. Soil-aggregate size contents under different erosion positions. The error bars are three standard errors of the means (n = 3). $PSA_{1–4}$, the percentage contents of 2–5, 0.25–2, 0.053–0.25 mm and <0.053 mm aggregates, respectively; WSA, the percentage content of >0.25 mm water-stable aggregate. UC: upper catchment; CW: collapsing wall; CD: colluvial deposit; SC: scour channel; AF: alluvial fan. Different capital and lowercase letters indicate different erosion positions, and aggregate sizes are significant at $p < 0.05$, respectively.

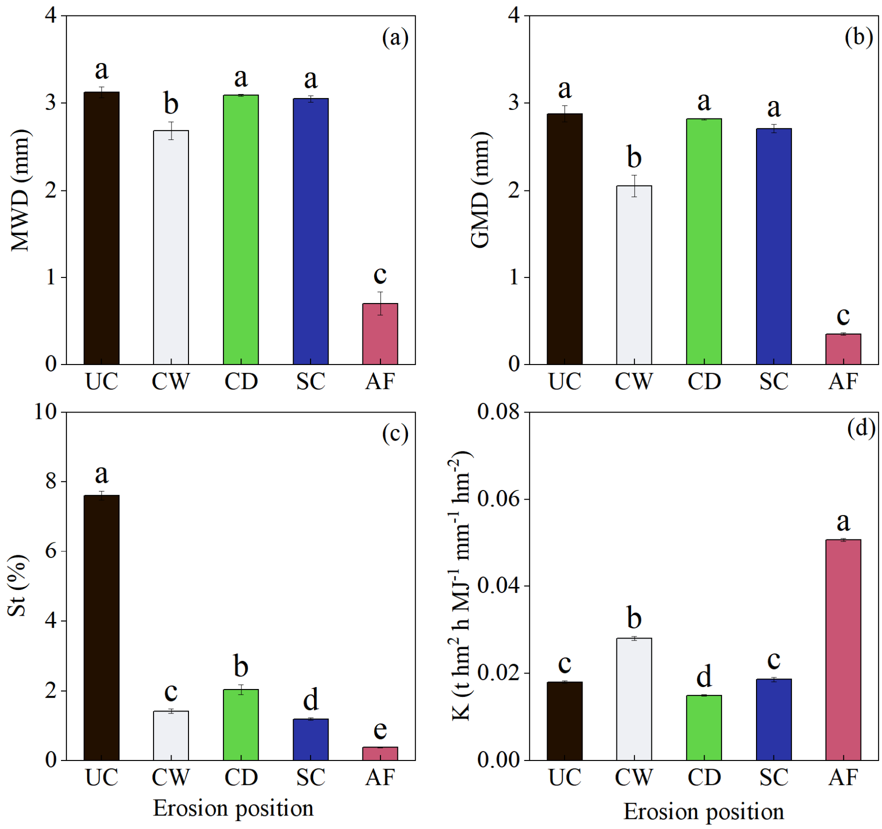

Figure 3. Soil aggregate stability indexes: (**a**) represents the values of mean weight diameter (MWD) under the five erosion positions; (**b**) represents the values of the geometric mean diameter (GMD) under the five erosion positions; (**c**) represents the values of the soil structural stability index (St) under the five erosion positions; and (**d**) represents the values of the erodibility factor (K) under the five erosion positions. The error bars represent the standard errors of three means (n = 3). UC: upper catchment; CW: collapsing wall; CD: colluvial deposit; SC: scour channel; AF: alluvial fan. Different lowercase letters indicate the significant differences among different erosion positions ($p < 0.05$).

3.3. Changes in Labile OC Fraction and C Pool Management Index along Erosion Positions

Soil erosion significantly influenced soil labile-C fractions, pools, and management indices at different positions (Figures 4 and 5, $p < 0.05$). The NLOC ranged from 1.1–23.9 g kg^{-1} and dominated the C fractions by 74.2–75.9% (Figure 4a). Compared with UC, LLOC, MLOC, HLOC, and NLOC contents significantly decreased by 2.00–2.07 g kg^{-1}, 3.93–4.16 g kg^{-1}, 1.62–1.75 g kg^{-1} and 21.80–22.82 g kg^{-1} at the CW, CD, SC, and AF positions, respectively (Figure 4a, $p < 0.05$). Moreover, the lower content of each labile C-fraction was detected at the CD and SC positions as compared to the rest of the positions (Figure 4b). Similarly, passive-C dominated the soil C pool rather than labile-C across different positions (Figure 4b). Soil passive-C was significantly lower at AF than at the UC, CW, CD and SC positions, which was opposite to labile-C (Figure 4b, $p < 0.05$).

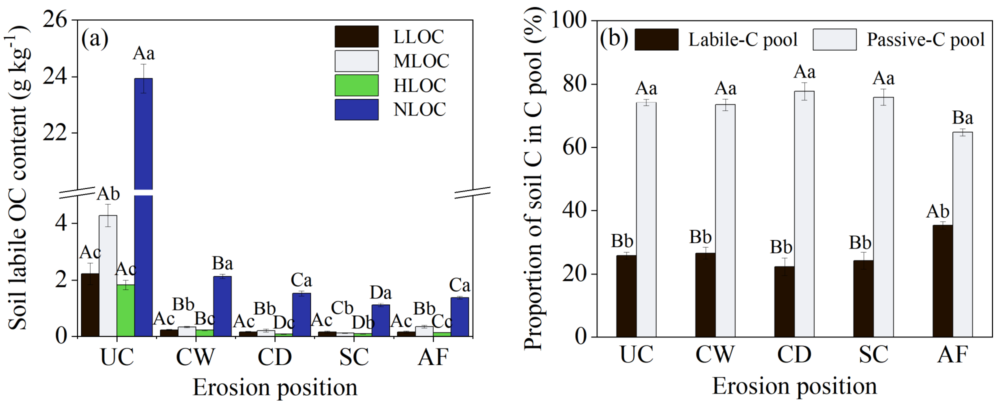

Figure 4. Soil organic carbon (SOC) fractions: (**a**) represents the contents of soil labile organic carbon (LOC) under the five erosion positions; and (**b**) represents the proportion of soil C in the C pool under the five erosion positions. The error bars represent the standard errors of three means (n = 3). LLOC: less-labile organic C; MLOC: moderately labile organic C; HLOC: high-labile organic C; NLOC: non-labile organic C; UC: upper catchment; CW: collapsing wall; CD: colluvial deposit; SC: scour channel; AF: alluvial fan. Different capital and lower-case letters indicate a significant difference among erosion positions and soil LOC fractions or C pools, respectively ($p < 0.05$).

Compared with UC, the CPI values were significantly lower in the range of 1.88–1.97 at the CW, CD, SC, and AF positions (Figure 5a). In addition, we found that there were coincident changes between the L and LI values in the order of AF > SC > CD, CW, and UC, with the values of 0.09–0.21 and 0.21–0.46, respectively (Figure 5b,c). The CPMI was significantly higher at UC than at CW, CD, SC, and AF, with an increment of 36.9–39.9% (Figure 5d, $p < 0.05$).

3.4. Relationship among Soil Properties, Labile-OC Pool Indexes and Soil-Aggregate Stability

Our study showed that soil properties had a significant correlation with soil C pool management indexes and aggregate stability (Table 2, $p < 0.05$). Soil labile-C correlated considerably positively with silt and CP and significantly negatively with sand, while soil passive-C had an opposite trend with labile-C (Table 2, $p < 0.01$). Moreover, L and LI had a positive correlation with silt (Table 2, $p < 0.01$). Similarly, the MWD, GMD and WSA had a positive correlation with sand, but a negative correlation with silt and CP (Table 2, $p < 0.01$), while K had a significantly positive association with silt and CP but a substantially negative association with the Fea and sand contents (Table 2, $p < 0.01$). Moreover, LLOC, MLOC, HLOC, NLOC, CPI, CPMI and St values correlated substantially positively with TN, Fef and clay contents (Table 2, $p < 0.01$).

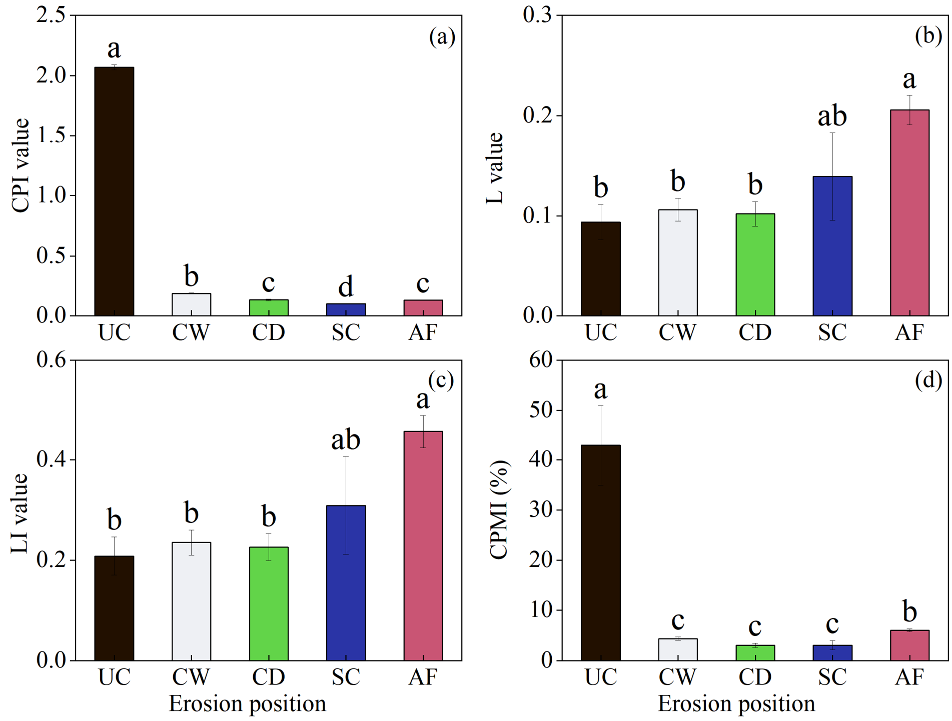

Figure 5. Characteristics of soil C pool management: (**a**) represents the values of the C pool index (CPI) under the five erosion positions; (**b**) represents the values of the C pool liability (L) under the five erosion positions; (**c**) represents the values of the C pool lability index (LI) under the five erosion positions; and (**d**) represents the values of soil C pool management index (CPMI) under the five erosion positions. The error bars represent the standard errors of three means (n = 3). UC: upper catchment; CW: collapsing wall; CD: colluvial deposit; SC: scour channel; AF: alluvial fan. Different lower-case letters indicate a significant difference among erosion positions ($p < 0.05$).

Table 2. Correlation coefficients among soil properties, aggregate stability, LOC fractions and C pool indexes under different erosion positions (n = 15). Correlation coefficients among soil-aggregate stability, erodibility, LOC fractions and C pool indexes under different erosion positions (n = 15).

Variables	BD	CP	Sand	Silt	Clay	TN	Fef	Fea
MWD	0.441	−0.948 **	0.730 **	−0.989 **	0.008	0.308	0.470	0.396
GMD	0.465	−0.969 **	0.682 **	−0.984 **	0.075	0.362	0.509	0.265
WSA	0.440	−0.944 **	0.739 **	−0.993 **	−0.001	0.307	0.473	0.444
K	−0.386	0.921 **	−0.756 **	0.980 **	0.044	−0.270	−0.443	−0.546 *
St	−0.169	−0.543	−0.245	−0.441	0.878 **	0.977 **	0.985 **	−0.058
SOC	−0.297	−0.406	−0.416	−0.276	0.953 **	0.996 **	0.975 **	−0.101
LLOC	−0.376	−0.369	−0.447	−0.217	0.933 **	0.951 **	0.921 **	−0.134
MLOC	−0.286	−0.362	−0.441	−0.239	0.948 **	0.986 **	0.957 **	−0.115
HLOC	−0.361	−0.402	−0.424	−0.261	0.946 **	0.987 **	0.964 **	−0.075
NLOC	−0.287	−0.407	−0.411	−0.280	0.950 **	0.996 **	0.976 **	−0.098
Labile-C	−0.498	0.697 *	−0.726 **	0.832 **	0.166	−0.105	−0.243	−0.268
Passive-C	0.498	−0.697 *	0.726 **	−0.832 **	−0.166	0.105	0.243	0.268
CPI	−0.297	−0.405	−0.417	−0.276	0.953 **	0.996 **	0.975 **	−0.102
L	−0.082	0.562	−0.430	0.711 **	−0.151	−0.392	−0.507	−0.393
LI	−0.058	0.542	−0.434	0.701 **	−0.132	−0.370	−0.484	−0.401
CPMI	−0.381	−0.359	−0.453	−0.205	0.929 **	0.943 **	0.910 **	−0.141

MWD, mean weight diameter; GMD, geometric mean diameter; WSA, the percentage content of > 0.25 mm water-stable aggregate; K, soil erodibility factor; St, soil structural stability index; SOC, soil organic C; LLOC, less-labile organic C; MLOC, moderately labile organic C; HLOC, high-labile organic C; NLOC, non-labile organic C; CPI, C pool index; L, C pool liability; LI, C pool liability index; CPMI, C pool management index. BD, bulk density; CP, capillary porosity; TN, total N; Fef, free iron; Fea, amorphous iron oxide. The * and ** represent the significant difference at $p < 0.05$ and $p < 0.01$, respectively.

Correlation analysis revealed that soil OC, LLOC, MLOC, HLOC and NLOC values were all positively correlated with CPMI, with the determination coefficient of 0.95, 1.00, 0.90, 0.98, and 0.94, respectively (Figure 2, $p < 0.01$). Furthermore, we found that soil LLOC, MLOC, HLOC, NLOC, CPI and CPMI values were all positively correlated with St (Table 2, $p < 0.05$), while those indexes had no correlation with MWD, GMD, WSA and K (Table 2, $p > 0.05$). Inversely, soil labile-C, L and LI had a negative correlation with MWD, GMD and WSA, and positive correlation with K. However, passive-C had a significantly positive correlation with MWD, GMD and WSA, and had a significantly negatively correlation with K (Table 2, $p < 0.05$).

Principal component analysis (PCA) displayed that soil physicochemical properties were greatly correlated with C pool indexes (Figure 6a) and aggregate stability (Figure 6b). The erosion sites from the CW, SC and CD were positioned on the PCA plane's bottom side. In contrast, the AF and UC positions were on the left and right sides of the PCA, respectively (Figure 6a,b). Furthermore, we explored the influence of soil characteristics and LOC fractions on aggregate stability using RDA (Figure 7). According to Table 3, the first two axes of RDA explained 98.9% (Figure 7), with silt (82.3%), SOC (16.1%) and Fea (0.80%) contributing. Moreover, soil-aggregate stability indices, including MWD, GMD, and WSA, were favorably connected to SOC and Fea but were negatively related to silt by RDA (Figure 7).

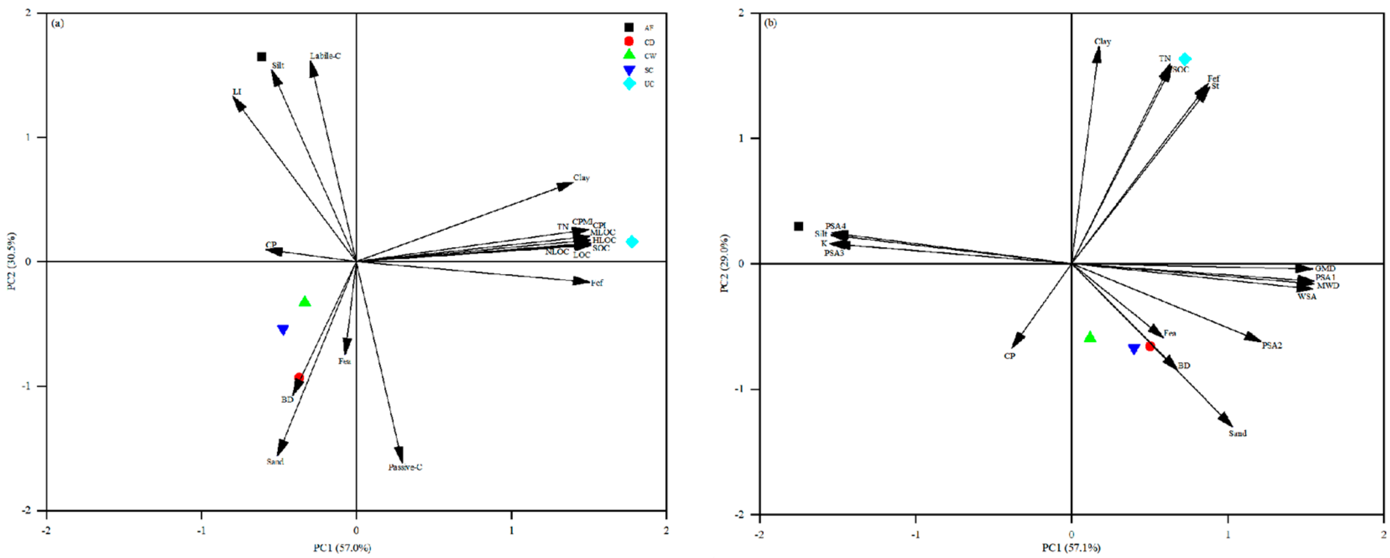

Figure 6. Principal component analysis (PCA) and scores plotted in the plane of PC1 and PC2: (**a**) represents PCA between soil basic properties and C pool indexes; and (**b**) represents PCA between soil basic properties and aggregate stability indexes. SOC, soil organic carbon; TN, total nitrogen; Fef, free iron; Fea, amorphous iron oxide; BD, bulk density; CP, capillary porosity; LLOC, less-labile organic C; MLOC, moderately labile organic C; HLOC, high-labile organic C; NLOC, non-labile organic C; CPI, C pool index; L, C pool liability; LI, C pool lability index; CPMI, C pool management index; PSA_{1-4}, the percentage contents of 2−5, 0.25−2, 0.053−0.25 mm and <0.053 mm aggregates, respectively; MWD, mean weight diameter; GMD, geometric mean diameter; WSA, the percentage content of >0.25 mm water-stable aggregate; St, structural stability index; K, soil erodibility factor; UC, upper catchment; CW, collapsing wall; CD, colluvial deposit; SC, scour channel; AF, alluvial fan.

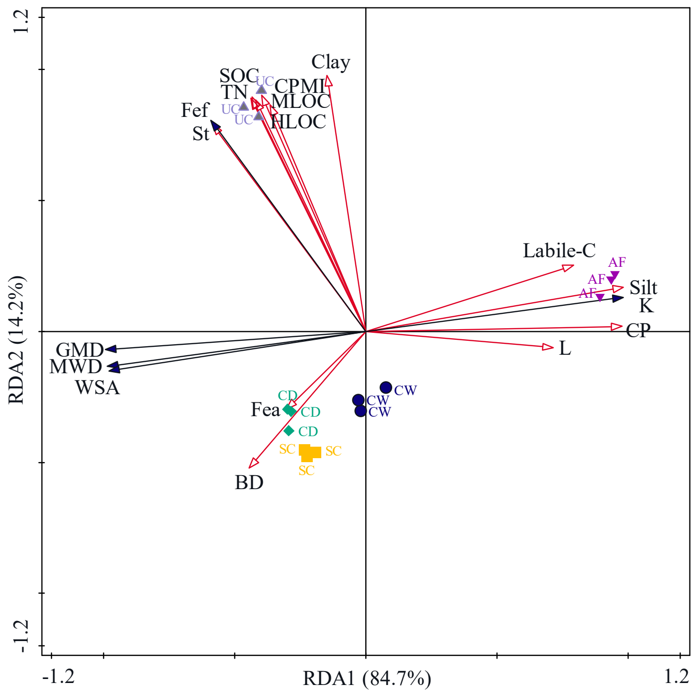

Figure 7. Two-dimensional sequence diagram of redundancy analysis (RDA) among soil properties, labile organic C fractions and aggregate stability at different erosion positions. SOC, soil organic carbon; TN, total nitrogen; Fef, free iron; Fea, amorphous iron oxide; BD, bulk density; CP, capillary porosity. MLOC, moderately labile organic C; HLOC, high-labile organic C; NLOC, non-labile organic C; CPI, the C pool index; L, the C pool liability; LI, the C pool lability index; CPMI, the C pool management index. PSA_{1-4}, the percentage contents of 2−5, 0.25−2, 0.053−0.25 mm and <0.053 mm aggregates, respectively; MWD, mean weight diameters; GMD, geometric mean diameter; WSA, the percentage content of >0.25 mm water-stable aggregate; St, structural stability index; K, soil erodibility factor. UC, upper catchment; CW, collapsing wall; CD, colluvial deposit; SC, scour channel; AF, alluvial fan.

Table 3. Two-dimensional explanation of redundancy analysis (RDA) among soil properties, labile organic C fractions and aggregate stability at different erosion positions.

Variables	Explains (%)	Pseudo-F	*p*
Silt	82.3	60.4	0.002
SOC	16.1	122.0	0.002
Fea	0.80	10.0	0.002
Clay	0.20	2.70	0.080
Fef	<0.1	1.30	0.242
BD	<0.1	0.80	0.432
MLOC	<0.1	0.40	0.650
HLOC	<0.1	0.50	0.584
CP	<0.1	0.60	0.502
Labile-C	<0.1	0.20	0.808
L	0.10	1.10	0.348
TN	0.20	6.80	0.126
CPMI	<0.1	0.40	0.560
Statistic		Axis 1	Axis 2
Eigenvalues		0.8474	0.1425
Explained variation (cumulative)		84.74	98.98
Pseudo-canonical correlation		0.9999	0.9999
Explained fitted variation (cumulative)		84.78	99.03

SOC, soil organic C; Fea, amorphous iron oxide; Fef, free iron; BD, bulk density; MLOC, moderately labile organic C; HLOC, high-labile organic C; CP, capillary porosity; L, the C pool liability; TN, total N; CPMI, the C pool management index.

4. Discussion

4.1. Relationship among Soil Properties, Labile OC Pool Indexes and Aggregate Stability

Soil organic C pools are primarily dependent on the balance between the input from crop and root decomposition, and the outflow from mineralization and the leaching/runoff process, which change soil LOC fractions [1]. In our study, the soil of UC position had higher LLOC contents compared with the rest of the positions (Figure 4), which was attributed to the losses of SOC and nutrients by flow during the erosion process [54]. Moreover, AF soil had a significantly higher labile-C content and lower passive-C content compared with higher positions. This is because passive organic C dominated the SOC, which can accelerate during the aggregation of microaggregate to macroaggregate [27]. Since AF soil was strongly affected by the deposition of sediments transported from higher positions by gravity, it has more microaggregates and lower aggregate stability [13], further causing the low passive OC.

Integrating soil organic C pool and lability into soil CPMI may give a readily available index to assess agricultural management methods' ability to enhance soil quality [55,56]. We found that the soil CPI had a trend of decline along erosion positions. Still, soil L and LI were opposite (Figure 5a–c), which were correlated with the SOC changes (Table 1). In addition, the CPMI was highest at the UC position among all the erosion positions (Figure 5d), indicating that soil quality had a declining trend along with the height of the collapsing-gully erosion positions. Moreover, soil buildup and vertical migration below the erosion position increased the SOC content at the AF position.

Additionally, the lateral SOC migration downslope dominated vertical translocation at the CW, CD, and SC positions, increasing SOC at the UC position (Table 1). This is probably because erosion-induced soil reallocation generated a large redistribution of SOC and further resulted in the degradation of soil quality along the slope [57]. According to Van Oost et al. (2007), topsoil erosion might cause variations in the vertical distribution and the storage-soil labile and recalcitrant organic C pools [58]. Therefore, collapsing-gully erosion can change soil C pool quality and heterogeneity by affecting the distributions of SOC and LOC fractions in our study.

4.2. Soil-Aggregate Size and Stability at Different Erosion Positions

Our research found that soil-aggregate content and aggregate stability significantly differed among erosion positions (Figures 2 and 3). The AF soil has lower PSA_1 and PSA_2 contents but higher PSA_3 and PSA_4 contents (Figure 2), which indicates collapsing-gully erosion can reduce soil macroaggregates [46]. Moreover, the values of WSA, MWD and GMD at the UC, CW, CD and SC positions were higher than those in AF (Figures 2 and 3), indicating that the soil has lower aggregate stability at the AF position. This is because natural rainfall breaks soil macroaggregates into microaggregates, which move into the AF position with rainfall runoff [54], further increasing the <0.25 mm aggregate contents (Figure 2), thus causing the lower aggregate stability of AF soil. Similarly, AF soil had a lower St but higher K value than the rest of erosion positions (Figure 3c,d), indicating AF soil had poor structural stability and easily suffered from erosion under collapsing-gully erosion conditions. These results are probably because of the fast development of the collapsing gully being governed by the retreat of the UC and the collapse of the CW, the base-level of erosion controlling the re-erosion of the colluvial deposit, and the development speed [59]. Those processes could generate the redistribution of soil materials at various positions, which cause the loss of the small soil particle and nutrients, as well as the descending of soil-structure stability along the direction of overland runoff [44]. However, the change in the natural environment directly triggered collapsing-gully formation due to human activities [60].

Additionally, rainfall infiltration could increase soil weights, which drove soil collapse, and further caused soil leaching and thus reduced the soil stability and anti-erosion ability [19]. Furthermore, soil particles and associated organic C could be transported from the initial eroding site (UC) to the depositional site (AF) along the slope [61], which resulted in the elution of base ions and the loss of cementing materials (e.g., iron oxides), and further affected the structural instability of AF soil. Therefore, frequent rainfall erosion could weaken soil aggregate stability and lead to a loss in soil quality and function, threatening the ecosystem's stability.

4.3. Effects of Soil Basic Parameters and LOC Pool Indexes on Aggregate Stability

Soil properties and LOC pool indexes had a positive correlation with soil-aggregate stability (Tables S2 and S3, Figure 6), which indicates that collapsing-gully erosion could change the stability of LOC pool and soil properties by maintaining better soil structure, further improving soil quality [53,56]. In our study, clay content was positively correlated with St (Table 2). Moreover, sand had a positively correlation with MWD, GMD and WSA (Table 2 and Figure 6a), which is possibly because clay is mainly used as a bonding agent and interacted with cations and organic compounds in soil [62], and further promoted soil-aggregate formation. Moreover, silt could strongly affect aggregate stability by changing the soil size composition and thus affecting soil structure [63]. Meanwhile, soil Fea and SOC significantly contributed to aggregate stability (Figure 7 and Table 2), because Fea and SOC could accelerate aggregate formation [64], especially under collapsing-gully erosion conditions. In contrast, L and LI had a negative effect on MWD, GMD, and WSA (Table 2 and Figure 6b), indicating that soil has a great capacity for improving soil-aggregate stability by the stability of LOC pool [50,65]. These results were perhaps because the CPMI response to collapsing-gully erosion was consistent with the changes of SOC and LOC fractions [66].

Our study also found that SOC and all soil LOC fractions were positively correlated with CPMI (Figure S1), indicating that SOC content was an incredibly significant driver of the amount of LOC pool existing [67]. Furthermore, a linear relationship was found between soil properties, including SOC, TN, Fef, and clay, and labile C fractions (Table 2). Furthermore, soil LOC pools could improve the soil quality, possibly affecting soil properties in our study. Therefore, soil LOC fractions might be vital parameters of the direction and amount of soil organic C cycling and the stability of the soil structure, and even the soil quality, after collapsing-gully erosion.

5. Conclusions

This research provided insight into the impacts of soil LOC pools on aggregate stability across the different positions of collapsing-gully erosion in the Acric Ferralsols region of south China. Collapsing-gully erosion significantly affected aggregate stability and labile C pool quality. Although the range of responses of different soil LOC fractions and aggregate stability to different erosion positions were different, UC soil had higher MWD, GMD, WSA, St, LOC fractions, CPI, and CPMI, which indicates that the stable C pool (passive-C) contributed to the increases in soil-aggregate stability. Furthermore, SOC, silt, and Fea contents significantly affected aggregate stability. At the same time, those indexes significantly correlated with soil LOC pool indexes, which further indicated that the combined actions among soil LOC fractions, C pool and soil characteristics affected aggregate stability. The soil labile C pool was a valuable indication of soil structure and quality following soil erosion. Therefore, the decreases in the contents of soil LOC fractions were mostly attributable to soil-structure depletion, which resulted in changes in soil properties during erosion. Moreover, our research suggests that the improving aggregate stability induced by rainfall erosion is required to preserve soil LOC pool stability and increase SOC input in China's south subtropical Acric Ferralsols region.

Supplementary Materials: The following supporting information can be downloaded at: https://www.mdpi.com/article/10.3390/agronomy13071869/s1, Figure S1: Pearson's correlation coefficients among soil organic C, labile C fractions and C pool management index under different soil erosion positions; Table S1: Basic chemical properties in soil aggregate of the study sites (mean ± SE); Table S2: Loading factors of parameters on the first Principal Components (PC1 and PC2) of principal component analysis (PCA) applied to physicochemical parameters and labile C fractions of soils subject to erosion positions; Table S3: Comprehensive scores of labile C stability with different erosion positions; Table S4: Loading factors of parameters on the first Principal Components (PC1 and PC2) of principal component analysis (PCA) applied to physicochemical parameters, aggregate stability and erodibility of soils subject to erosion positions; Table S5: Comprehensive scores of labile C stability with different erosion positions.

Author Contributions: Conceptualization, methodology, writing—original draft preparation, B.L. and Y.L.; investigation, visualization, writing—original draft preparation, X.T.; visualization, formal analysis, Y.A.H., H.S., J.Z., J.W. and T.Z.; writing—review and editing, X.T. and H.W.; funding acquisition, Y.L. All authors have read and agreed to the published version of the manuscript.

Funding: This research was funded by the National Natural Science Foundation of China (42277290) and the National Key Research and Development Project of China (2022YFD2301402).

Data Availability Statement: The data presented in this study are available on request from the corresponding author.

Conflicts of Interest: The authors declare no conflict of interest.

References

1. Yuan, G.Y.; Huan, W.W.; Song, H.; Lu, D.J.; Chen, X.Q.; Wang, H.Y.; Zhou, J.M. Effects of straw incorporation and potassium fertilizer on crop yields, soil organic carbon, and active carbon in the rice-wheat system. *Soil Tillage Res.* **2021**, *209*, 104958. [CrossRef]
2. Alhaj Hamoud, Y.; Shaghaleh, H.; Wang, R.k.; Franz Gouertoumbo, W.; Ali Adam Hamad, A.; Salah Sheteiwy, M.; Wang, Z.C.; Guo, X.P. Wheat straw burial improves physiological traits, yield and grain quality of rice by regulating antioxidant system and nitrogen assimilation enzymes under alternate wetting and drying irrigation. *Rice Sci.* **2022**, *29*, 473–488. [CrossRef]
3. Poeplau, C.; Katterer, T.; Leblans, N.I.W.; Sigurdsson, B.D. Sensitivity of soil carbon fractions and their specific stabilization mechanisms to extreme soil warming in a subarctic grassland. *Glob. Chang. Biol.* **2017**, *23*, 1316–1327. [CrossRef] [PubMed]
4. Yang, X.; Zhang, K.; Shaghaleh, H.; Qi, Z.; Gao, C.; Chang, T.; Zhang, J.; Zia-ur-Rehman, M.; Hamoud, Y.A. Continuous cropping alters soil hydraulic and physicochemical properties in the Karst region of southwestern China. *Agronomy* **2023**, *13*, 1416. [CrossRef]
5. Saha, M.; Das, M.; Sarkar, A. Distinct nature of soil organic carbon pools and indices under nineteen years of rice based crop diversification switched over from uncultivated land in eastern plateau region of India. *Soil Tillage Res.* **2021**, *207*, 104856. [CrossRef]
6. Xiao, L.; Yao, K.; Li, P.; Liu, Y.; Chang, E.; Zhang, Y.; Zhu, T. Increased soil aggregate stability is strongly correlated with root and soil properties along a gradient of secondary succession on the Loess Plateau. *Ecol. Eng.* **2020**, *143*, 105671. [CrossRef]
7. Haynes, R.J. Labile organic matter fractions as central components of the quality of agricultural soils: An overview. *Adv. Agron.* **2005**, *85*, 221–268.
8. Ghorbani, M.; Neugschwandtner, R.W.; Soja, G.; Konvalina, P.; Kopecký, M. Carbon Fixation and Soil Aggregation Affected by Biochar Oxidized with Hydrogen Peroxide: Considering the Efficiency of Pyrolysis Temperature. *Sustainability* **2023**, *15*, 7158. [CrossRef]
9. Li, H.Q.; Zhu, H.S.; Liang, C.L.; Wei, X.R.; Yao, Y.F. Soil erosion significantly decreases aggregate-associated OC and N in agricultural soils of Northeast China. *Agric. Ecosyst. Environ.* **2022**, *323*, 107677. [CrossRef]
10. Jat, S.L.; Parihara, C.M.; Singha, A.K.; Nayak, H.S.; Meena, B.R.; Kumara, B.; Pariharc, M.D.; Jat, M.L. Differential response from nitrogen sources with and without residue management under conservation agriculture on crop yields, water-use and economics in maize-based rotations. *Field Crops Res.* **2019**, *236*, 96–110. [CrossRef]
11. Tisdall, J.M.; Oades, J.M. Organic matter and water-stable aggregates in soils. *Eur. J. Soil Sci.* **1982**, *33*, 141–163. [CrossRef]
12. Abiven, S.; Menasseri, S.; Chenu, C. The effects of organic inputs over time on soil aggregate stability—A literature analysis. *Soil Biol. Biochem.* **2009**, *41*, 1–12. [CrossRef]
13. Wei, Y.J.; Liu, Z.; Wu, X.L.; Zhang, Y.; Cui, T.T.; Cai, C.F.; Guo, Z.L.; Wang, J.G.; Cheng, D.B. Can benggang be regarded as gully erosion? *Catena* **2021**, *207*, 105648. [CrossRef]
14. Müller-Nedebock, D.; Chaplot, V. Soil carbon losses by sheet erosion: A potentially critical contribution to the global carbon cycle. *Earth Surf. Proc. Land.* **2015**, *40*, 1803–1813. [CrossRef]
15. Nie, X.D.; Li, Z.W.; He, J.J.; Huang, J.Q.; Zhang, Y.; Huang, B.; Ma, W.M.; Lu, Y.M.; Zeng, G.M. Enrichment of organic carbon in sediment under field simulated rainfall experiments. *Environ. Earth Sci.* **2015**, *74*, 5417–5425. [CrossRef]
16. Lützow, M.V.; Kögel-Knabner, I.; Ekschmitt, K.; Matzner, E.; Guggenberger, G.; Marschner, B.; Flessa, H. Stabilization of organic matter in temperate soils: Mechanisms and their relevance under different soil conditions- a review. *Eur. J. Soil Sci.* **2006**, *57*, 426–445. [CrossRef]
17. Wang, X.; Cammeraat, L.H.; Wang, Z.; Zhou, J.; Govers, G.; Kalbitz, K. Stability of organic matter in soils of the Belgian Loess Belt upon erosion and deposition. *Eur. J. Soil Sci.* **2013**, *64*, 219–228. [CrossRef]

18. Deng, Y.S.; Duan, X.Q.; Ding, S.W.; Cai, C.F. Effect of joint structure and slope direction on the development of collapsing gully in tuffaceous sandstone area in South China. *Int. Soil Water Conse.* **2020**, *8*, 131–140. [CrossRef]
19. Ji, X.; Thompson, A.; Lin, J.S.; Jiang, F.S.; Ge, H.L.; Yu, M.M.; Huang, Y.H. Modeling spatial distribution of rainfall infiltration amounts in South China using cellular automata and its relationship with the occurrence of collapsing gullies. *Catena* **2020**, *194*, 104676. [CrossRef]
20. Xia, D.; Deng, Y.S.; Wang, S.L.; Ding, S.W.; Cai, C.F. Fractal features of soil particle-size distribution of different weathering profiles of the collapsing gullies in the hilly granitic region, south China. *Nat. Hazards* **2015**, *79*, 455–478. [CrossRef]
21. Chen, J.L.; Zhou, M.; Lin, J.S.; Jiang, F.S.; Huang, B.F.; Xu, T.T. Comparison of soil physicochemical properties and mineralogical compositions between noncollapsible soils and collapsed gullies. *Geoderma* **2018**, *317*, 56–66. [CrossRef]
22. Borrelli, P.; Robinson, D.A.; Fleischer, L.R.; Lugato, E.; Ballabio, C.; Alewell, C.; Meusburger, K.; Modugno, S.; Schütt, B.; Ferro, V.; et al. An assessment of the global impact of 21st century land use change on soil erosion. *Nat. Commun.* **2017**, *8*, 2013. [CrossRef] [PubMed]
23. Santos, R.S.; Wiesmeier, M.; Cherubin, M.R.; Oliveira, D.M.S.; Locatelli, J.L.; Holzschuh, M.; Cerri, C.E.P. Consequences of land-use change in Brazil's new agricultural frontier: A soil physical health assessment. *Geoderma* **2021**, *400*, 115149. [CrossRef]
24. Smith, R.W.; Bianchi, T.S.; Allison, M.; Savage, C.; Galy, V. High rates of organic carbon burial in fjord sediments globally. *Nat. Geosci.* **2015**, *8*, 450–453. [CrossRef]
25. Mendonça, R.; Müller, R.A.; Clow, D.; Verpoorter, C.; Raymond, P.; Tranvik, L.J.; Sobek, S. Organic carbon burial in global lakes and reservoirs. *Nat. Commun.* **2017**, *8*, 1694. [CrossRef]
26. Blanco-Moure, N.; Gracia, R.; Bielsa, A.C.; Lopez, M.V. Soil organic matter fractions as affected by tillage and soil texture under semiarid Mediterranean conditions. *Soil Tillage Res.* **2016**, *155*, 381–389. [CrossRef]
27. Li, T.T.; Zhang, Y.L.; Bei, S.K.; Li, X.L.; Reinsch, S.; Zhang, H.Y.; Zhang, J.L. Contrasting impacts of manure and inorganic fertilizer applications for nine years on soil organic carbon and its labile fractions in bulk soil and soil aggregates. *Catena* **2020**, *194*, 104739. [CrossRef]
28. Liu, C.; Li, Z.W.; Chang, X.F.; He, J.J.; Nie, X.D.; Liu, L.; Xiao, H.B.; Wang, D.Y.; Peng, H.; Zeng, G.M. Soil carbon and nitrogen sources and redistribution as affected by erosion and deposition processes: A case study in a loess hilly-gully catchment, China. *Agric. Ecosyst. Environ.* **2018**, *253*, 11–22. [CrossRef]
29. Zhang, K.L.; Yu, Y.; Dong, J.; Yang, Q.; Xu, X. Adapting & testing use of USLE K factor for agricultural soils in China. *Agric. Ecosyst. Environ.* **2019**, *269*, 148–155. [CrossRef]
30. Chen, S.Q.; Zhang, G.H.; Luo, Y.F.; Zhou, H.; Wang, K.W.; Wang, C.S. Soil erodibility indicators as affected by water level fluctuations in the Three Gorges Reservoir area, China. *Catena* **2021**, *207*, 105693. [CrossRef]
31. Wang, H.; Zhang, G.H.; Li, N.N.; Zhang, B.J.; Yang, H.Y. Variation in soil erodibility under five typical land uses in a small watershed on the Loess Plateau, China. *Catena* **2019**, *174*, 24–35. [CrossRef]
32. Abbas, F.; Zhu, Z.L.; An, S.S. Evaluating aggregate stability of soils under different plant species in Ziwuling Mountain area using three renowned methods. *Catena* **2021**, *207*, 105616. [CrossRef]
33. Krausea, L.; Klumpp, E.; Nofz, I.; Missong, A.; Amelung, W.; Siebers, N. Colloidal iron and organic carbon control soil aggregate formation and stability in arable Luvisols. *Geoderma* **2020**, *374*, 11421. [CrossRef]
34. Franz Gouertoumbo, W.; Alhaj Hamoud, Y.; Guo, X.; Shaghaleh, H.; Ali Adam Hamad, A.; Elsadek, E. Wheat Straw Burial Enhances the Root Physiology, Productivity, and Water Utilization Efficiency of Rice under Alternative Wetting and Drying Irrigation. *Sustainability* **2022**, *14*, 16394. [CrossRef]
35. Zhaoqing Municipal Bureau of Statistics. *Zhaoqing Statistical Yearbook 2022*; Zhaoqing Municipal Bureau of Statistics: Zhaoqing, China, 2022.
36. Zhou, H.Y.; Li, H.X.; Ye, Q.; Wu, G.W. Simulation of morphological development of soil cracks in the collapsing hill region of southern China. *Res. Soil Water Conserv.* **2016**, *23*, 338–342.
37. Soil Survey Staff. *Keys to Soil Taxonomy*, 11th ed.; USDA Natural Resources Conservation Service: Washington, DC, USA, 2010.
38. Tang, X.; Qiu, J.C.; Xu, Y.Q.; Li, J.H.; Chen, J.H.; Li, B.; Lu, Y. Responses of soil aggregate stability to organic C and total N as controlled by land-use type in a region of south China affected by sheet erosion. *Catena* **2022**, *218*, 106543. [CrossRef]
39. Forster, J.C. Soil sampling, handling, storage and analysis. In *Methods in Applied Soil Microbiology and Biochemistry*; Alef, K., Nannipieri, P., Eds.; Academic Press: Pittsburgh, CA, USA, 1995; Part 3; pp. 49–121. [CrossRef]
40. Zhao, J.S.; Chen, S.; Hui, R.G.; Li, Y.Y. Aggregate stability and size distribution of red soils under different land uses integrally regulated by soil organic matter, and iron and aluminum oxides. *Soil Tillage Res.* **2017**, *167*, 73–79. [CrossRef]
41. Elliott, E.T. Aggregate structure and carbon, nitrogen, and phosphorus in native and cultivated soils. *Soil Sci. Soc. Am. J.* **1986**, *50*, 627–633. [CrossRef]
42. Lu, J.; Zheng, F.L.; Li, G.F.; Bian, F.; An, J. The effects of raindrop impact and runoff detachment on hillslope soil erosion and soil aggregate loss in the Mollisol region of Northeast China. *Soil Tillage Res.* **2016**, *161*, 79–85. [CrossRef]
43. Zhu, G.Y.; Shang-Guan, Z.P.; Deng, L. Soil aggregate stability and aggregate-associated carbon and nitrogen in natural restoration grassland and Chinese red pine plantation on the Loess Plateau. *Catena* **2017**, *149*, 253–260. [CrossRef]
44. Zheng, J.Y.; Zhao, J.S.; Shi, Z.H.; Wang, L. Soil aggregates are key factors that regulate erosion-related carbon loss in citrus orchards of southern China: Bare land vs. grass-covered land. *Agric. Ecosyst. Environ.* **2021**, *309*, 107254. [CrossRef]

45. Tagar, A.A.; Adamowski, J.; Memon, M.S.; Do, M.C.; Mashori, A.S.; Soomro, A.S.; Bhayo, W.A. Soil fragmentation and aggregate stability as affected by conventional tillage implements and relations with fractal dimensions. *Soil Tillage Res.* **2020**, *197*, 104494. [CrossRef]
46. Wei, Y.J.; Cai, C.F.; Guo, Z.L.; Wang, J.G. Linkage between aggregate stability of granitic soils and the permanent gully erosion in subtropical China. *Soil Tillage Res.* **2022**, *221*, 105411. [CrossRef]
47. Reynolds, W.D.; Drury, C.F.; Tan, C.S.; Fox, C.A.; Yang, X.M. Use of indicators and pore volume-function characteristics to quantify soil physical quality. *Geoderma* **2009**, *152*, 252–263. [CrossRef]
48. Zhang, K.L.; Shu, A.P.; Xu, X.L.; Yang, Q.K.; Yu, B. Soil erodibility and its estimation for agricultural soils in China. *J. Arid Environ.* **2008**, *72*, 1002–1011. [CrossRef]
49. Lefroy, R.D.B.; Blair, G.; Strong, W.M. Changes in soil organic matter with cropping as measured by organic carbon fractions and 13C natural isotope abundance. *Plant Soil* **1993**, *155–156*, 399–402. [CrossRef]
50. Xu, M.; Lou, Y.; Sun, X.; Wang, W.; Baniyamuddin, M.; Zhao, K. Soil organic carbon active fractions as early indicators for total carbon change under straw incorporation. *Biol. Fert. Soils* **2011**, *47*, 745–752. [CrossRef]
51. Yang, X.; Drury, C.F.; Wander, M.M. A wide view of no-tillage practices and soil organic carbon sequestration. *Acta Agric. Scand. Sect. B-Soil Plant Sci.* **2013**, *63*, 523–530. [CrossRef]
52. Murphy, R.P.; Montes-Molina, J.A.; Govaerts, B.; Six, J.; Kessel, C.; Fonte, S.J. Crop residue retention enhances soil properties and nitrogen cycling in smallholder maize systems of Chiapas, Mexico. *Appl. Soil Ecol.* **2016**, *103*, 110–116. [CrossRef]
53. Blair, G.; Lefroy, R.; Lisle, L. Soil carbon fractions based on their degree of oxidation, and the development of a carbon management index for agricultural systems. *Aust J. Agric. Res.* **1995**, *46*, 1459–1466. [CrossRef]
54. Li, Y.; Mo, Y.Q.; Are, K.S.; Huang, Z.G.; Guo, H.; Tang, C.; Abegunrin, T.P.; Qin, Z.H.; Kang, Z.W.; Wang, X. Sugarcane planting patterns control ephemeral gully erosion and associated nutrient losses: Evidence from hillslope observation. *Agric. Ecosys. Environ.* **2021**, *309*, 107289. [CrossRef]
55. Vieira, F.C.B.; Bayer, C.; Zanatta, J.A.; Dieckow, J.; Mielniczuk, J.; He, Z.L. Carbon management index based on physical fractionation of soil organic matter in an Acrisol under long-term no-till cropping systems. *Soil Tillage Res.* **2007**, *96*, 195–204. [CrossRef]
56. Wang, W.; Lai, D.Y.F.; Wang, C.; Pan, T.; Zeng, C. Effects of rice straw incorporation on active soil organic carbon pools in a subtropical paddy field. *Soil Tillage Res.* **2015**, *152*, 8–16. [CrossRef]
57. Doetterl, S.; Six, J.; Van-Wesemael, B.; Van-Oost, K. Carbon cycling in eroding landscapes: Geomorphic controls on soil organic C pool composition and C stabilization. *Glob. Chang. Biol.* **2012**, *18*, 2218–2232. [CrossRef]
58. Van Oostt, K.; Quineg, T.A.; Goverss, G.; De Gryzej, S.; Six, J.; Harden, J.W.; Ritchie, J.C.; Mccarty, G.W.; Heckrath, G.; Kosmas, C.; et al. The impact of agricultural soil erosion on the global carbon cycle. *Science* **2007**, *318*, 626–629. [CrossRef]
59. Deng, Y.S.; Cai, C.F.; Xia, D.; Ding, S.W.; Chen, J.Z.; Wang, T.W. Soil atterberg limits of different weathering profiles of the collapsing gullies in the hilly granitic region of Southern China. *Solid Earth* **2017**, *8*, 499–513. [CrossRef]
60. Amundson, R.; Berhe, A.A.; Hopmans, J.W.; Olson, C.; Sztein, A.E.; Sparks, D.L. Soil and human security in the 21st century. *Science* **2015**, *348*, 1261071. [CrossRef]
61. Li, Y.; Quine, T.A.; Yu, H.Q.; Govers, G.; Six, J.; Gong, D.Z.; Van-Oost, K. Sustained high magnitude erosional forcing generates an organic carbon sink: Test and implications in the Loess Plateau, China. *Earth Planet. Sci. Lett.* **2015**, *411*, 281–289. [CrossRef]
62. Fink, J.R.; Inda, A.V.; Bavaresco, J.; Barrón, V.; Torrent, J.; Bayer, C. Phosphorus adsorption and desorption in undisturbed samples from subtropical soils under conventional tillage or no-tillage. *J. Plant Nutr. Soil Sc.* **2016**, *179*, 198–205. [CrossRef]
63. Paradelo, R.; Van-Oort, F.; Chenu, C. Water-dispersible clay in bare fallow soils after 80 years of continuous fertilizer addition. *Geoderma* **2013**, *200–201*, 40–44. [CrossRef]
64. Xue, B.; Huang, L.; Huang, Y.N.; Zhou, F.L.; Li, F.; Ali-Kubar, K.; Li, X.K.; Lu, J.W.; Zhu, J. Roles of soil organic carbon and iron oxides on aggregate formation and stability in two paddy soils. *Soil Tillage Res.* **2019**, *187*, 161–171. [CrossRef]
65. Ghosh, B.N.; Meena, V.S.; Alam, N.M.; Dogra, P.; Bhattacharyya, R.; Sharma, N.K.; Mishra, P.K. Impact of conservation practices on soil aggregation and the carbon management index after seven years of maize-wheat cropping system in the Indian Himalayas. *Agric. Ecosys. Environ.* **2016**, *216*, 247–257. [CrossRef]
66. Šimanskýa, V.; Juriga, M.; Jonczak, J.; Uzarowicz, Ł.; Stępień, W. How relationships between soil organic matter parameters and soil structure characteristics are affected by the long-term fertilization of a sandy soil. *Geoderma* **2019**, *342*, 75–84. [CrossRef]
67. Gong, W.; Yan, X.; Wang, J.; Hu, T.; Gong, Y. Long-term manure and fertilizer effects on soil organic matter fractions and microbes under a wheat-maize cropping system in northern China. *Geoderma* **2009**, *149*, 318–324. [CrossRef]